Evaluating Microelectrode Arrays in Peripheral Nerve Using Micro Computed Tomography*

Rebecca A. Frederick, *Student Member, IEEE*, Ryan Margolis, *Student Member, IEEE*, Kenneth Hoyt, *Senior Member, IEEE*, and Stuart F. Cogan, *Member, IEEE*

***Abstract*— Many advances have been made with imaging of implanted neural devices; however, the ability to image whole nerve samples remains limited. Further, few imaging modalities are well suited for visualizing both whole devices *in vivo* and individual microelectrodes within a nerve. In this study, we used micro-computed tomography (micro-CT) to evaluate Wireless Floating Microelectrode Arrays (WMFAs) implanted in rat sciatic nerve at the level of whole devices and individual electrodes. WFMAs were also used to track selective recruitment of plantar flexion and dorsiflexion of the rear paw, which was achieved by each implanted device (*n=6*) during chronic implantation. Evoked limb motion was correlated to end-of-study assessments using micro-CT to visualize electrode locations within the fascicular structure of the sciatic nerve. Results of this study show that micro-CT imaging can provide valuable assessments of microelectrode arrays implanted in peripheral nerves for both whole devices visualized *in vivo* and individual electrodes visualized in whole nerve tissue samples.**

***Clinical Relevance*— This work informs the use of micro-computed tomography as a tool for correlating neural device performance with physical attributes of the implant location.**

I. Introduction

Previous studies have investigated devices implanted in peripheral nerves for a variety of neural engineering applications, especially those related to nerve regeneration, neural recording, and neural stimulation. In studies of microelectrode arrays (MEAs) implanted for recording or stimulation, quantifying of the location of microelectrodes within or surrounding the nerve is critical for accurately interpreting most study outcomes. In particular, the ability to locate electrodes within nerves that have axons organized into distinct fascicles can allow direct correlation of motor or sensory related study outcomes to implant locations.

Current methods for visualizing microelectrode arrays implanted in peripheral nerves usually include surgical microscope images taken during the implantation procedure along with histological assessments of neural tissue after the conclusion of the study when implanted devices are removed. Tissue processing techniques for histology try to capture the location of each implanted electrode within thin slices of neural tissue, but this is not always possible and failure to capture an electrode within a tissue section typically results in the loss of any information on relative position of the electrode to structures within the nerve. It is therefore advantageous to be able to image whole nerve samples and guarantee the ability to visualize the location of every electrode within an array.

Most recently, developments in tissue clearing techniques have proven to be useful for visualizing the 3-dimensional structure of whole organs and tissues. [1-3] Tissue clearing can provide high resolution images of neural tissue and cellular structures near an electrode array while maintaining the overall tissue structure; however, tissue clearing can be expensive and time consuming to complete and has the potential to lead to contraction or expansion of the tissue, [3] distorting spatial relationships. Where cellular resolution is not immediately necessary, micro-computed tomography (micro-CT) can provide high resolution images of whole nerve samples for visualizing many types of implanted microelectrode arrays. Micro-CT allows imaging at ultra-high resolution up to 30 µm, which would allow visualization of fascicles within peripheral nerves. [4] Techniques developed by S. Pixley et al. [5,6] show that micro-CT can be used to visualize the fascicular structure of peripheral nerves relative to an implanted device, while still allowing the use of many common tissue processing methods for histological analysis.

In this study, we present the use of micro-CT imaging to help visualize wireless devices implanted in the sciatic nerve of Sprague Dawley rats. Position of the telemetry coil for Wireless Floating Microelectrode Arrays (WFMAs) was evaluated using micro-CT to visualize animal to animal variability and aid positioning of the external telemetry coil for device communication. Chronic performance of WFMAs was evaluated by tracking the type of motion elicited and required current thresholds when applying constant-current stimulation pulses to each electrode in the implanted array. After study completion, the excised sciatic nerve was separated from the WFMA and stained with a contrast agent. Then, micro-CT imaging was used again to correlate electrode position within the nerve to the previously recorded measures of motor recruitment and chronic stimulation performance.

II. Methods

All animal procedures were performed in accordance with the guidelines of the Institutional Animal Care and Use Committee of The University of Texas at Dallas.

A. Neural Stimulation Device Design

The design of wireless floating microelectrode arrays was described in prior work. [7-9] In summary, WFMAs consist of

*Research supported by Texas CPRIT RP180670 (K. Hoyt) and a gift through Vanguard Charitable (S. F. Cogan).

R. A. Frederick, R. Margolis, K. Hoyt, and S. F. Cogan are with the Bioengineering Department at The University of Texas at Dallas, Richardson, TX 75080 USA. Corresponding author: R. A. Frederick (e-mail: rebecca.frederick@utdallas.edu).

3 main components: a ceramic substrate and ASIC, iridium microwire electrodes, and a telemetry coil. The microelectrode array consisted of 2 uninsulated electrodes (reference and counter) and 16 Parylene-insulated activated iridium oxide film (AIROF) electrodes [9] with an exposed surface area of 2000 μm^2. Electrode microwires were 100 µm in diameter (tapered at the tip) and had alternating lengths of 650 µm and 850 µm, with 400 µm center-to-center spacing (electrode layout shown in Fig. 1). WFMAs were encapsulated with silane-enhanced PDMS and then placed inside a silicone channel to help keep devices in-place on the sciatic nerve.

B. Device Implantation

10- to 16-week-old female Sprague Dawley rats (*n=6*, Charles River Labs, Wilmington, MA) were anesthetized with inhaled isoflurane (2.0-3.0%) and the left hind limb was shaved and cleaned with 10% povidone-iodine and 70% alcohol. An incision was made in the skin parallel to the left femur. The biceps femoris muscle was separated from gluteus superficialis and vastus lateralis by spreading the connective tissue between the muscles, and biceps femoris was then retracted to reveal the sciatic nerve. The nerve was detached from the surrounding tissue by separating the connective tissue around the entire circumference of the nerve until an exposed length of approximately 1.2 cm was achieved.

The WFMA was then placed under the nerve so that the flat coil surface rested on the underlying muscle tissue, and the nerve was placed on top of the electrodes inside the silicone channel. The left sciatic nerve and WFMA were then carefully pressed together until electrodes penetrated the sciatic nerve. The device was secured in place using a silicone sealant (Kwik-Cast™). Fig. 1 shows an implanted WFMA device after it was secured with silicone sealant (green). The muscle was then closed with 4-0 silk suture and the skin closed with 11 mm suture clips. Animals were given slow release buprenorphine immediately after surgery and every 72 hours as needed for 1 week thereafter to manage post-op pain. Animals were also given cefazolin antibiotic immediately after surgery and water with sulfamethoxazole *ad libitum* for one week post-op as a prophylactic.

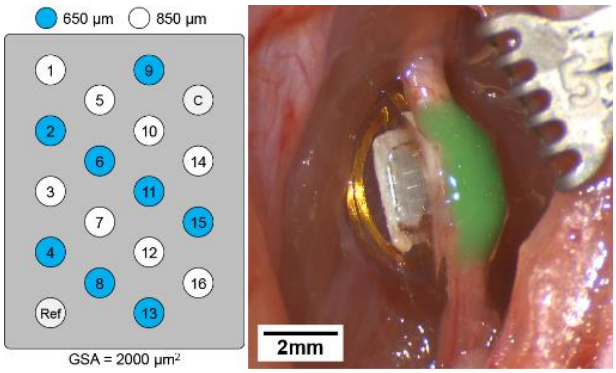

Figure 1. (Left) Microelectrode array layout with electrode lengths indicated by blue (650 µm) or white (850 µm) shading. (Right) WFMA secured with Kwik-Cast™ silicone sealant (green) after implantation in the left sciatic nerve.

C. Tracking Limb Motion

Neural stimulation trials were performed under isoflurane anesthesia (1.0-2.0%) once per week for 8 weeks and then once every 2 weeks for the remainder of the 38-week study. Stimulation trials were completed for the full 38-week study period for one animal to date. Animals were positioned on an elevated surface such that the left hind limb was free to move without restriction. The external wireless telemetry coil was positioned over the implanted device, and motion of the limb was recorded with two Stingray F033C IRF CSM video cameras (Allied Vision Technologies GmbH, Germany) at 80 frames per second. Each electrode was tested individually with 200.2 µs pulses at 1 Hz, gradually increasing the current in increments of 2 to 10 µA until either reaching the maximum output of the device or observing a 1 Hz twitch in the left paw that was clearly distinguishable from motion caused by breathing. The threshold current (I_{th}) for generating a visible twitch was recorded for each electrode. Limb motion for each electrode was classified as either plantar flexion or dorsiflexion using video recordings of each applied stimulus.

D. Visualizing Device Orientation

Ultra-high-resolution micro-CT imaging (OI/CT, MILabs, Utrecht, Netherlands) was performed to visualize the position of the WFMA relative to the neighboring skeletal structure. Scanning was completed under isoflurane anesthesia (2.0-2.5%) on post-op day 196, 106, 133, 120, 106, and 105 for animal A01, A02, A03, A04, A05, and A06 respectively. Animals were scanned using an accurate, ultra-focus magnification using a quarter degree step angle at one projection per step and a binning size of 1 for a total of 1440 frames. Image acquisition occurred at a voltage of 50 kV, a current of 0.21 mA, and an exposure of 75 ms. Images were reconstructed using vendor software and converted to DICOM (Digital Imaging and Communications in Medicine) files using PMOD analysis software (PMOD Technologies LLC, Zurich, Switzerland) at a voxel size of 30 µm. DICOM files were then imported into OsiriX (Pixmeo, Bernex, Switzerland) for post-processing analysis. Implants were visualized using the Mass Intensity Projection (MIP) 3D Viewer.

E. Sciatic Nerve Extraction, micro-CT, and Histology

At this time, animal A01 is the only subject that has reached the final study time point of 38 weeks post-implantation. At the end of the study period, final stimulation testing was completed, and the animal was euthanized with sodium pentobarbital overdose followed by perfusion with 0.9% saline then with 4% paraformaldehyde (PFA) in 1x phosphate buffered saline (PBS). The sciatic nerve was removed from the right (contralateral) limb and the left (implanted) limb with the WFMA kept in place, and both nerves were post-fixed in 4% PFA at 4°C for 48 hours. After fixation, nerve tissue was stored at 4°C in 1x PBS.

Tissue surrounding the excised nerve samples was removed by blunt dissection under a surgical microscope. For the implanted nerve, the silicone sealant (green) was removed, and then the nerve was carefully pulled away from the WFMA. The left (implanted) sciatic nerve was then stained with 2% Lugol's iodine solution (Thermo Fisher Scientific, "Lugol's solution, dilute" 6% total iodine, item #S99481) for 48 hours at room temperature to provide contrast for micro-CT. [5] The sciatic nerve was placed in 1x PBS inside a 3D printed holder (Fig. 2) placed in the mouse bed attachment in the center of the micro-CT while the detector rotates 360° around the sample. Imaging was completed with the same parameters described for visualizing device orientation, but with a 0.100-degree step

angle for a total of 3600 frames. Pre-processing and file conversion procedures were performed in the same manner as described above for the implanted WFMAs. However, DICOM files were imported into OsiriX (Pixmeo, Bernex, Switzerland) for 3D volume rendering. Images were manually adjusted using the 16-bit Color Look-Up Table (CLUT) to optimize the rendered 3D images. After micro-CT imaging, the left sciatic nerve was placed in 2.5% sodium thiosulfate (STS) solution (SigmaAldrich, item #217263) for 48 hours at room temperature to remove iodine from the tissue. [5] The nerve was then returned to 1x PBS at 4°C for storage until beginning paraffin embedding, tissue sectioning, and staining.

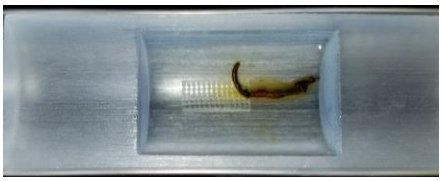

Figure 2. Top-down view of implanted (left) sciatic nerve placed inside a custom 3D printed holder with 1x PBS after staining.

III. Results and Discussion

A. Visualizing Devices in Vivo

The location and orientation of WFMAs was easily identified using micro-CT without any contrast agents. However, the position of the electrodes within the nerve is not visible *in vivo* without adding contrast to the nerve tissue. We were able to use micro-CT to visualize electrode positions within the nerve only after tissue extraction, as the contrast agent used is not suitable for *in vivo* application. Future work will need to develop suitable contrast agents for visualizing nerve fascicles *in vivo* using micro-CT. Reconstruction of micro-CT images of the whole nerve and implanted electrodes can be accomplished in as little as 5 minutes. And so, the addition of a suitable contrast agent would open the door for use of micro-CT as a tool for mapping and targeting tissue structures during device implantation.

Resulting 3D reconstruction of the device imaged *in vivo* (Fig. 3) was able to resolve individual electrodes and was used to determine if any one electrode was bent or broken after device implantation. The relative position of the implanted telemetry coil was also easily identified and was used to understand animal-to-animal variability of device orientation. The ability to visualize the telemetry coil *in vivo* after healing of the surgical site can also help improve alignment of the external coil for consistent communication with the implanted WFMA and improved data recording via reverse-telemetry.

Other imaging methods such as magnetic resonance imaging (MRI) or ultrasound imaging may provide similar information about the position of microelectrode arrays implanted in peripheral nerves. Future work should compare results of micro-CT to other imaging methods for visualizing neural devices, especially those with wireless communication components. Additionally, visualizing the vasculature near implanted neural devices would be valuable information for evaluating surgical trauma and chronic response to device implantation. And so, future work will investigate the use of contrast agents with micro-CT imaging for visualizing the vasculature near implanted WFMAs compared to the contralateral (non-implanted) limb.

While micro-CT imaging was able to resolve the MEA used in this study, the ability to visualize implanted microelectrodes with cross-section dimensions smaller than 100 μm will need to be tested further. In theory, micro-CT imaging should allow *in vivo* visualization of microelectrodes with dimensions as small as 30 μm, [4] but this will depend on the type of materials used to fabricate the MEA and whether or not there is enough contrast difference between the implanted electrodes and surrounding tissues to visualize the MEA with micro-CT imaging.

B. Motor Activation Patterns and Electrode Position

Plantar flexion and dorsiflexion of the left hind limb was evoked by constant-current stimulation in all six implanted animals, and the type of motion evoked by each electrode did not change through the first 8 weeks post-implantation. For the one animal that has completed the 38-week study period (A01), video recordings of evoked limb motion were correlated to electrode positions using micro-CT imaging of the excised sciatic nerve. Fascicular structure of the sciatic nerve along with the location of the implanted electrodes was distinguishable using only 2% Lugol's solution for contrast. Fig. 4 shows the 3D reconstruction of the whole nerve sample at the location of the implanted WFMA.

Fig. 5 shows selected images of the cross-section of the nerve generated by micro-CT with visible tracts for each electrode. Electrodes that evoked limb motion at the final study day (week 38) are labeled with the threshold current required for visible motion of the limb. Electrodes located completely within a nerve fascicle (E05, E08, E09, E11, E12, and E13) had much lower current thresholds (4.1 to 10.8 μA) than those located between fascicles (E06 at 20.3 μA and E07 at 44.7 μA) or at the outer edge of the nerve (E02 at 60.3 μA). Electrodes evoking plantar flexion throughout the study (E01, E02, E03, E04, E05, E06, E07, and E08) were located within or near the sciatic nerve fascicle corresponding to the tibial nerve. Similarly, electrodes evoking dorsiflexion throughout the study (E09, E11, E12, and E13) were located within or near the sciatic nerve fascicle corresponding to the peroneal nerve. Electrodes evoking no movement during the study (E14, E15, and E16) were located at the outer edge of the sciatic nerve, as seen upon visual inspection during device removal and later confirmed by micro-CT imaging. One electrode (E10) was non-functional at the time of implantation and no stimulation trials were completed for that electrode.

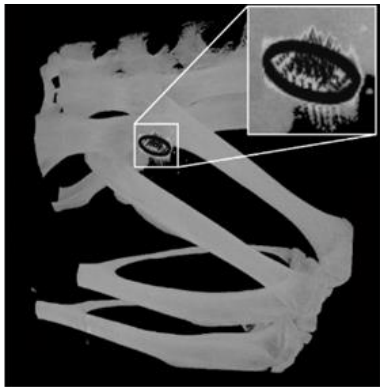

Figure 3. 3D reconstruction after micro-CT imaging of an implanted WFMA with the surrounding skeletal structure. Median plane view from the left side of animal A01.

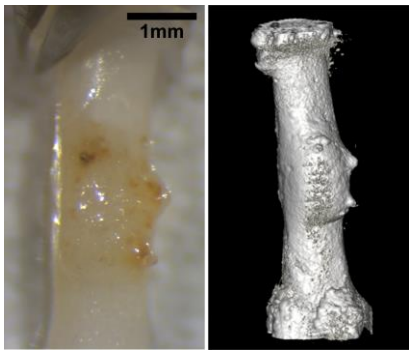

Figure 4. 3D reconstruction (right) from micro-CT imaging of the implanted sciatic nerve excised from animal A01 with an image of the nerve after removal of the WFMA (left).

Future work will investigate the correlation between the micro-CT images of electrode locations presented here and images of tissue sections from the same nerves after paraffin embedding, sectioning, and staining. Further, tissue sections will need be evaluated for differences in myelination and cellular structure near electrodes, proximal to the implanted WFMA, distal to the WFMA, and between the implanted and contralateral sciatic nerves. The combination of results from micro-CT and histology should also allow correlation of the distances between electrodes and axons to the current thresholds recorded throughout the 38-week study period.

IV. Conclusion

Our study found that micro-CT is a useful tool for visualizing microelectrode arrays implanted in peripheral nerve. Imaging with micro-CT allowed qualitative assessments of wireless microelectrode array orientation *in vivo* and could be useful for future studies to assess any mechanical changes in implanted devices over time. Further, visualizing the fascicular structure of the sciatic nerve using extracted whole tissue samples and micro-CT can provide valuable assessments of any rotation along the length of the nerve relative to an implanted device. Whole-nerve images obtained by micro-CT showed locations of electrodes within the fascicles of the sciatic nerve and were correlated to the recruitment thresholds for dorsiflexion and plantar flexion observed during chronic device implantation.

Acknowledgment

The authors would like to thank Girdhari Rijal, Ph.D. for assistance with micro-CT imaging procedures, and Philip R. Troyk, Ph.D. for providing WFMA devices as well as telemetry hardware and software.

References

[1] P. Ariel, "A beginner's guide to tissue clearing," *The International Journal of Biochemistry & Cell Biology*, vol. 84, 2017, pp. 35-39.

[2] K. Tainaka, T. C. Murakami, E. A. Susaki, M. Fukayama, A. Kakita, and H. R. Ueda, "Chemical landscape for tissue clearing based on hydrophilic reagents," *Cell Reports*, vol. 24, 2018, pp. 2196-2210.e9.

[3] D. S. Richardson and J. W. Lichtman, "Clarifying tissue clearing." *Cell*, vol. 162, no. 2, 2015, pp. 246-257.

[4] Manual – uCT – OI Serie 6, MILABS, Utrecht, Netherlands, pp. 20.

[5] T. M. Hopkins, A. M. Heilman, J. A. Liggett, K. LaSance, K. J. Little, D. B. Hom, D. M. Minteer, K. G. Marra, and S. K. Pixley, "Combining micro-computed tomography with histology to analyze biomedical implants for peripheral nerve repair," *Journal of Neuroscience Methods*, vol. 255, 2015, pp. 122–130.

[6] S. K. Pixley, T. M. Hopkins, K. J. Little, and D. B. Hom, "Evaluation of peripheral nerve regeneration through biomaterial conduits via micro-CT imaging," *Laryngoscope Investigative Otolaryngology*, vol. 1, no. 6, 2016, pp. 185–190.

[7] P. R. Troyk, D. E. A. Detlefsen, and G. A. D. DeMichele, "A multifunctional neural electrode stimulation ASIC using NeuroTalk™ interface," *2006 International Conference of the IEEE Engineering in Medicine and Biology Society*, New York, NY, 2006, pp. 2994-2997.

[8] S. F. Cogan, P. R. Troyk, J. Ehrlich, T. D. Plante, and D. E. Detlefsen, "Potential-biased, asymmetric waveforms for charge-injection with activated iridium oxide (AIROF) neural stimulation electrodes," *IEEE Transactions on Biomedical Engineering*, vol. 53, no. 2, Feb. 2006, pp. 327-332.

[9] Z. Hu, P. Troyk, G. DeMichele, K. Kayvani, and S. Suh, "Intrinsic activation of iridium electrodes over a wireless link," *2012 Annual International Conference of the IEEE Engineering in Medicine and Biology Society*, San Diego, CA, 2012, pp. 2788-2791.

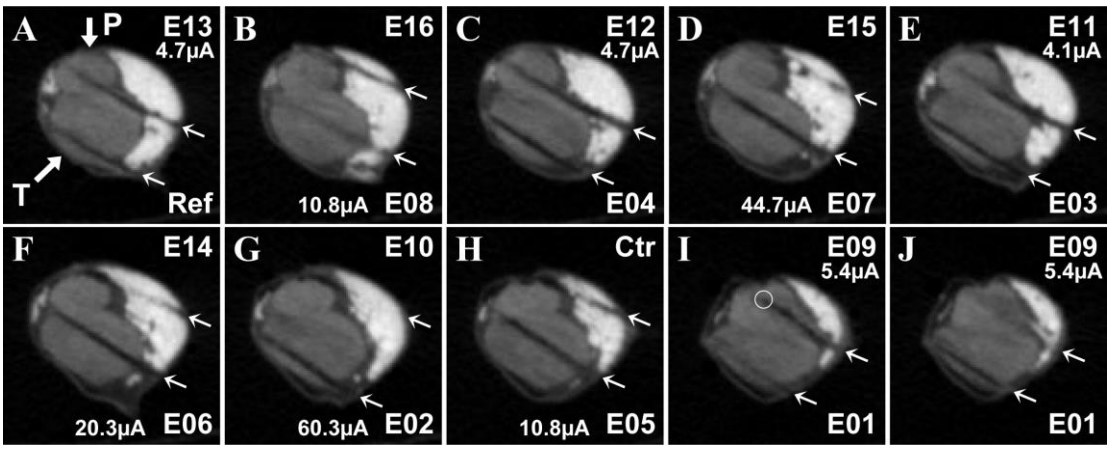

Figure 5. Selected cross-sections of the sciatic nerve generated by micro-CT imaging at the location of the implanted WFMA for animal A01. Panels A through J correspond to the most distal through most proximal electrodes, respectively. Microelectrodes are located at the very tip of each shaft. Panel I shows the approximate location of E09 circled in white. Tibial and peroneal nerve fascicles are indicated by the large white arrows (T and P) in panel A. Electrode insertion points are indicated by the small white arrows in each panel, where the top-most arrow corresponds to the electrode ID in the top right corner of the image and the bottom arrow corresponds to the electrode ID in the bottom right corner of the image. "Ref" is the reference electrode and "Ctr" is the counter electrode. All electrode ID's correspond to the layout in Fig. 1. Threshold currents for generating limb motion at the final day of testing are labeled next to the corresponding electrode ID. Those with no label did not evoke movement on the final day of testing.